WPMAT-PR(17) 17929

E. TEJADO et al.

Thermo-mechanical behaviour of W-Cu metal matrix composites for fusion heat sink applications: influence of the Cu content

Preprint of Paper to be submitted for publication in Journal of Nuclear Materials

This work has been carried out within the framework of the EUROfusion Consortium and has received funding from the Euratom research and training programme 2014-2018 under grant agreement No 633053. The views and opinions expressed herein do not necessarily reflect those of the European Commission.

Thermo-mechanical behaviour of W-Cu metal matrix composites for fusion heat sink applications: influence of the Cu content

E. Tejado[1], A. v. Müller[2,3], J-H. You[2], J.Y. Pastor[1]

[1] Departamento de Ciencia de Materiales-CIME, Universidad Politécnica de Madrid

C/ Profesor Aranguren 3, E28040-Madrid, Spain

[2]Max-Planck-Institut für Plasmaphysik, 85748 Garching, Germany

[3]Technische Universität Munchen, 85748 Garching, Germany

CORRESPONDING AUTHOR:
Elena Tejado
Departamento de Ciencia de Materiales-CIME, Universidad Politécnica de Madrid,
C/ Profesor Aranguren 3, E28040-Madrid, Spain.
Telephone: +34 913 365 243
Email: elena.tejado@mater.upm.es

Abstract

Copper and its alloys have been selected as heat sink materials for next generation fusion devices and will be joined to tungsten as armour material. However, the joint of W and Cu experiences high thermal stresses when exposed to high heat loads so an interlayer material could effectively ensure the lifetime of the component by reducing the thermal mismatch. Many researchers have published results on the production of W-Cu composites aiming attention at its thermal conductivity; nevertheless, the mechanical performance of these composites is still minor.

The present paper focuses on characterizing the thermo-mechanical material behaviour of W-Cu composites produced by means of liquid copper melt infiltration of porous W preform. This technique was applied to produce composites with 15, 30 and 40 wt. % Cu (36 %, *52 % and 76 % vol. %Cu)* The microstructure, thermal properties and mechanical performance were investigated and measured from room temperature up to 800 ºC. Results demonstrated that high densification and superior mechanical properties can be achieved through this manufacturing route. The mechanical properties (elastic modulus, fracture toughness and strength) of the composites show a certain dependency on the Cu content; fracture mode shifts from the dominantly brittle fracture of W particles with constrained deformation of the Cu phase at low Cu content to the predominance of the ductile fracture of Cu when its ratio is higher. Though strong degradation is observed at 800 ºC, mechanical properties at operation temperatures, i.e. below 350 ºC, remain rather high, and even better than other W/Cu materials reported previously.

In addition, it has been demonstrated that the elastic modulus and therefore, the coefficient of thermal expansion, can indeed be tailored through the control of W skeleton porosity. As a result, the W-Cu composite materials presented in this paper would successfully drive away heat produced in the fusion chamber, avoiding the mismatch between materials while contributing to the structural support of the system.

Keywords: Tungsten; Copper; Heat Sink; Mechanical Properties; High Temperature.

1. Introduction

Copper (Cu) and its alloys have been selected as heat sink materials for next generation fusion devices [1]. In order to ensure the correct heat transfer of the plasma facing components (PFCs), various combinations of joints between the armour and the heat sink have to be developed. Carbon fibres composites were selected firstly as plasma facing material for the strike point region of the initial ITER divertor installed for the non-tritium operational phase [2]. Though, only tungsten (W) and its alloys are currently considered for the next steps due to its high temperature mechanical properties but, specially, due to its low sputtering rate and low retention of tritium. As a result, the baseline model for the plasma-facing units of the divertor target plates is the ITER-type monoblock design, consisting of an array of tungsten armour monoblocks connected by a copper alloy (CuCrZr) cooling tube [3]. However, recent high heat flux qualification tests [4]and preliminary design studies of DEMO divertor target predict that CuCrZr could only meet the structural design requirements in a very narrow operation regime [5]. Therefore, advanced heat sink materials need to be developed for the improvement of the divertor target performance.

In addition, the joints between these components must withstand the thermal, mechanical and neutron loads under cyclic mode of operation, while providing high reliability during the lifecycle [6]. However, the joint of W and Cu endures high thermal stresses when exposed to high heat loads owing to the great difference of the coefficient of thermal expansion (CTE) and elastic modulus between them [7]. Moreover, W–Cu system has no mutual solubility and, therefore, the bonding strength at the interface is quite low. Functionally graded materials (FGMs), used as an interlayer, could effectively reduce the thermal stresses while ensuring the lifetime of the component [8]

[9]. Notwithstanding, the production of fully dense W-Cu FGMs is not a trivial issue. It is due not only due to the aforementioned properties mismatch, but also to the great difference between the melting points of W (approximately 3400 ºC) and Cu (approximately 1083 ºC), that make it difficult to produce a conventional alloy. To solve this problem, several authors have reported the beneficial effects of cobalt during the sintering process [10] and [11]. The addition of cobalt powder increases the wettability of W particles by Cu by forming the inter-metallic compound Co_7W_6, and thereby reducing the overall porosity in the structure and improving the mechanical properties of the final product [12]. Nonetheless, radioprotection requirements limit the presence of cobalt inside the reactor [13].

Among the preferred methods for producing fully dense W-Cu composites, laser [14] and plasma sintering [15] have gathered a lot of attention in the last few decades. However, the above processes are complex and the problem of adequate electrical conductivity of the powders and the achievement of homogenous temperature distribution is particularly acute [16]. Furthermore, homogeneous and dense W-rich composites (> 60 wt. % W) can only be produced by the infiltration technique [17]. In this synthesize route, a W skeleton with desired relative density is produced by powder metallurgy, compacted and sintered, and then the molten copper is infiltrated into the open pores of the W porous structure[18] [19].

In a previous paper [20], two W-based composites were manufactured with compositions of 30 wt. % Cu and 30 wt.% CuCrZr with homogeneous structure and high relative density through the infiltration technique. Results demonstrated that high densification, and superior mechanical properties, can be achieved through this producing route. Müller et al. [21] published a preliminary characterization of these W/

Cu products. Special focus was assessed on their thermal conductivity and its suitability as heat sink materials in PFCs of future nuclear fusion devices.

In the present research, we focused our interest in properly determining the effect of Cu content on the thermomechanical properties. Therefore, the above technique was applied to produce composites with 15 and 40 wt. % Cu, and the results have been compared with those obtained previously for W-30 wt. % Cu composites. The microstructure, thermal properties and mechanical performance were analysed and discussed.

2. Materials and methods

Commercial powders of tungsten with 8 μm size were used to produce a W skeleton consolidated by uniaxial cold pressing. The green specimens were sintered at 1150 ºC for 2 h in high purity hydrogen atmosphere. Sintered skeletons with desirable density, i.e. 85%, 70% and 60% (36 %, *52 % and 76 % pore volume fraction)*, were infiltrated by oxygen free molten copper. Infiltration was carried out at 1150 °C in hydrogen atmosphere for 2 h. Finally, specimens were machined to plates (3 mm x 30 mm x 150 mm) for later characterization. Three different compositions were produced with this technique: W-15wt.% Cu, W-30 wt.% Cu and W-40 wt.% Cu.

The density of the samples was measured using Archimedes' immersion method in high purity ethanol. The microstructure and fracture surfaces of the composites were characterized by Secondary Electron Microscopy (SEM, ZEISS AURIGA). Energy-Dispersive X-ray spectroscopy (EDX) attached in SEM was used to analyse the distribution of the W-Cu components.

From the composite materials, bend-test (2.8 mm×2.8 mm×30.0 mm) and tensile-test (dogbone-shape with 2.0 mm×2.5 mm ×17.0 mm of narrow portion) specimens were cut. Additionally, bend-test specimens were cut and notched with a femto-second laser for fracture toughness determination (Single-Edge-Laser-Notched-Bean, SELNB [22]). The mechanical characterization was carried out at the temperature range between 25 ºC and 800 ºC, in 125 ºC steps, under high vacuum (~10^{-6} mBar), and with a constant crosshead speed of 100 µm/min. Specimens were heated at 10 ºC/min and held at the test temperature for 15 min before testing. The reported values were the average of three measurements.

Bending strength and fracture toughness were obtained in three-point bending configuration with 25 mm span. The yield flexural strength was computed by Bernoulli equations for flexural beams with 0.2% of deformation. The K_{IQ} was calculated by the general expression of stress intensity factor [23] from the critical load (P_Q) and the beam section. The ASTM 5% secant method [24], i.e. a secant line with a slope equal to 95% of the initial elastic loading slope of the tangent line, was used to determine P_Q with an intention to define the K_{IQ} at the 2 % or less crack extension. Since linear elastic fracture mechanics is not valid when significant plastic deformation precedes failure [25], apparent values are given in the present work.

Tensile strength and true tensile stress-strain curves were obtained from Digital Image Correlation (DIC) of recorded tests. DIC uses image registration algorithms to track the relative displacements of material points between a reference image and a current image, hence instantaneous cross-sectional area can be obtained during each test. Constant volume was assumed during the tensile tests, hence 2D deformation setup was required and only one camera was needed. Since the tests were performed under high temperature and vacuum conditions (30 °C/min heating rate and 10 min dwell time under 10^{-6} mbar pressure), the experimental setup consisted of a high-resolution camera (3840 px x 2748 px) coupled with an adequate light source, recording through the window on the back side of the environmental chamber. To facilitate the DIC measurement, random speckle patterns were painted on the sample surface with a permanent marker. However, at temperatures above 600 °C only surface roughness, with its characteristic grayscale pattern, was used to calculate the displacement fields. Prior to the elevated temperature testing, a small mechanical load was applied to verify the symmetry of specimen. The further processing and measurement of the recorded displacement field was performed with the open source 2D DIC MATLAB based program Ncorr [26].

The elastic modulus at room temperature, was measured on prismatic samples using Resonance Frequency Analysis (RFA) technique. The slope change of the load and load-point displacement curves were used to study the evolution of the elastic modulus with temperature. From these values, it was possible to estimate the coefficient of thermal expansion.

3. Results and discussion

The relative densities of the sintered specimens, measured by Archimedes alcohol immersion method, revealed values of 91.5 %, 96.2 % and 94.3 % for W-15Cu, W-30Cu and W-40Cu, respectively. These results are in accordance with the ones published by other authors for W-Cu composites produced by the powder injection moulding method (relative density of 95.58 % with 20% Cu content [27]), but they are slightly lower than the ones obtained via microwave infiltration sintering method (relative density of 98.87% with 20 % Cu content)[28]. However, most of the researchers have reported the same tendency: with the increase in Cu fraction, internal pores infiltration and Cu migration becomes easier, which render filling of the pores inside the composite, thus increasing the density of the final product.

Fig. 1 shows the cross-section microstructure of polished and etched specimens of the W-Cu composites. The EDX mapping analysis shows that the green phase is W, while the surrounding red matrix is Cu. The microstructure shows that polyhedral W grains are distributed in the liquid phase Cu matrix while the solidified liquid phase is intertwined through the solid phase as a network.

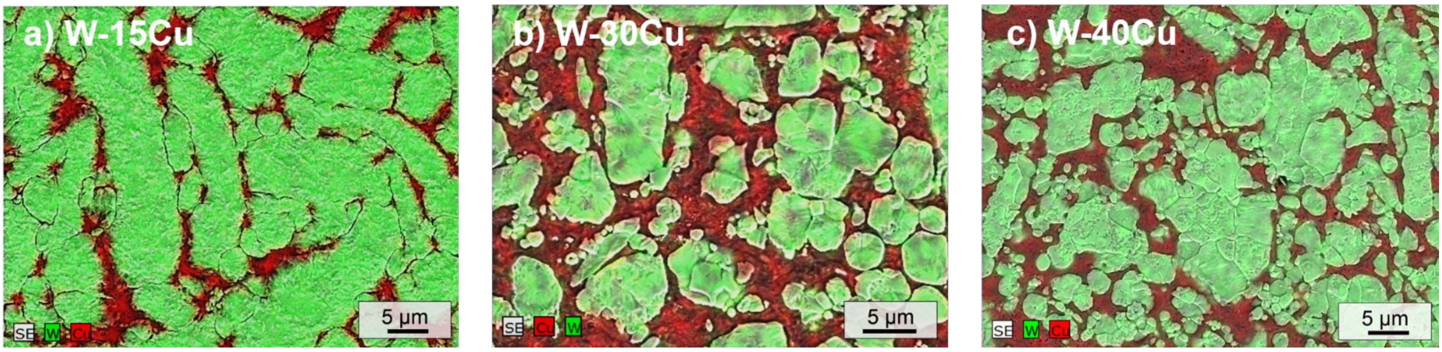

Fig. 1. SEM images with EDX detection of a)W-15wt.%Cu, b)W-30wt.%Cu and c) W-40wt.%Cu composites after metallographic preparation and etching.

On one hand, the difference among the microstructure observed for W-15Cu composite and the others is quite clear. Most of the grains observed at this magnification are W ones, and hence its average grain size is evidently larger than the observed for the other compounds. On the other hand, no clear differences can be extracted from Fig. 1 b) and c), even though the vol.% of Cu is slightly different, 48 vol.% Cu and 64 vol.% Cu, for W-30Cu and W-40Cu, respectively. In any case, these figures illustrate the contiguity and connective between the W solids, while the Cu-phases are apparently isolated in the matrix of tungsten, tough this is a continuous phase since it was produced by infiltration over the previous W scaffold. With the increase of Cu content, interconnection of the Cu-phases becomes much more frequent and, so that, the W–W grain contiguity decreases. Furthermore, the relative density measurements can be confirmed by the absence of visible pores in the Cu matrix.

- *Fracture toughness*

Fracture toughness values of the composites as a function of testing temperature are depicted in Fig. 2. It can be observed that there is an improvement in the fracture toughness when the Cu content decreases from 40 to 15 wt. % (Cu is a weak phase). In addition, a clear trend with temperature can be inferred from it. Fracture behaviour of W-30Cu and W-40Cu is quite similar, with values decreasing constantly with temperature. However, W-30Cu exhibits values on average 30 % higher than W-40Cu (16 MPa.$m^{1/2}$ versus 12 MPa.$m^{1/2}$ at 25 ºC). Nevertheless, this gap is narrower at high temperature, since both composites exhibit almost the same value at 800 ºC, 4.9 MPa $m^{1/2}$ and 6.0 MPa $m^{1/2}$. On the contrary, when temperature decreases, the effect of the low concentration of Cu (15 wt. % Cu) is more evident, as it reaches the highest value of fracture toughness at 425 ºC, ~ 19 MPa $m^{1/2}$. The softening of the W grain boundaries and the blunting of the crack tip may be the reason of this good mechanical behaviour [29]. Up to this temperature, Cu ductile phase controls the fracture and, thence, the degradation of the composite, showing values of around 9 MPa $m^{1/2}$, which in any case are much higher than the ones observed for the other materials tested.

Finally, the difference in toughness between materials at 800 ºC is clearly controlled by the percentage of W in the initial skeleton, as larger it is, higher is the exhibited toughness.

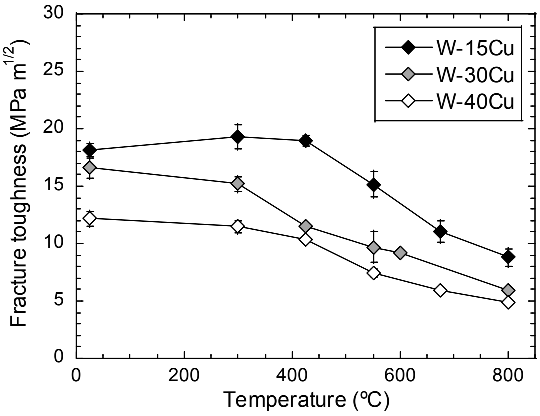

Fig. 2. Fracture toughness of the composites as a function of temperature and composition. Mean values and standard error

- *Flexural strength*

Fig. 3 shows the variation of flexural strength (0.2% yield strength) as a function of temperature. Yield strength increases with W content, reaching a maximum of 920 MPa at 25 ºC when Cu content is just 15 wt. %. Furthermore, the behaviour of the three materials is similar: bending strength decreases constantly with temperature with a relative rate of change between 0.55 and 0.70 MPa/ºC from 25 ºC to 800 ºC: from 920 MPa to 340 MPa for W-15Cu and from 480 MPa to 120 MPa for W-40Cu. As observed for fracture toughness, the flexural strength of W-30Cu and W-40Cu match closely, especially at high temperatures.

Also, it is worthily to mention that our results for W-15 wt.%Cu materials are quite better than the ones reported in literature for a W-20 wt.%Cu composite [30], with a bending strength of almost 800 MPa at 25 ºC. In addition, the sintering temperature of the aforementioned materials, 1250 ºC, is beyond the 1150 ºC of the ones in this study.

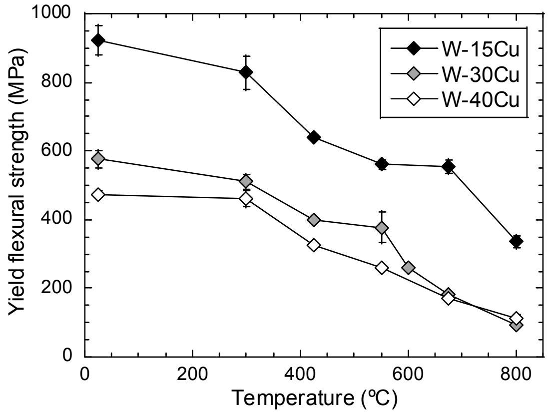

Fig. 3. Yield flexural strength as a function of temperature. Mean values and standard error

- *Tensile strength*

Fracture behaviour of W-Cu composites can be better observed in Fig. 4 where the true stress-strain curves of the tensile tests are represented. Real displacement as a function of temperature was obtained throw DIC analysis with resolutions higher than 10 μm/pixel. It should be however mentioned that the determination of the elastic displacements is a complex and difficult task, especially for Cu-rich samples where the necessary pre-load may cover this region and, so that, significant imprecisions may appear occasionally.

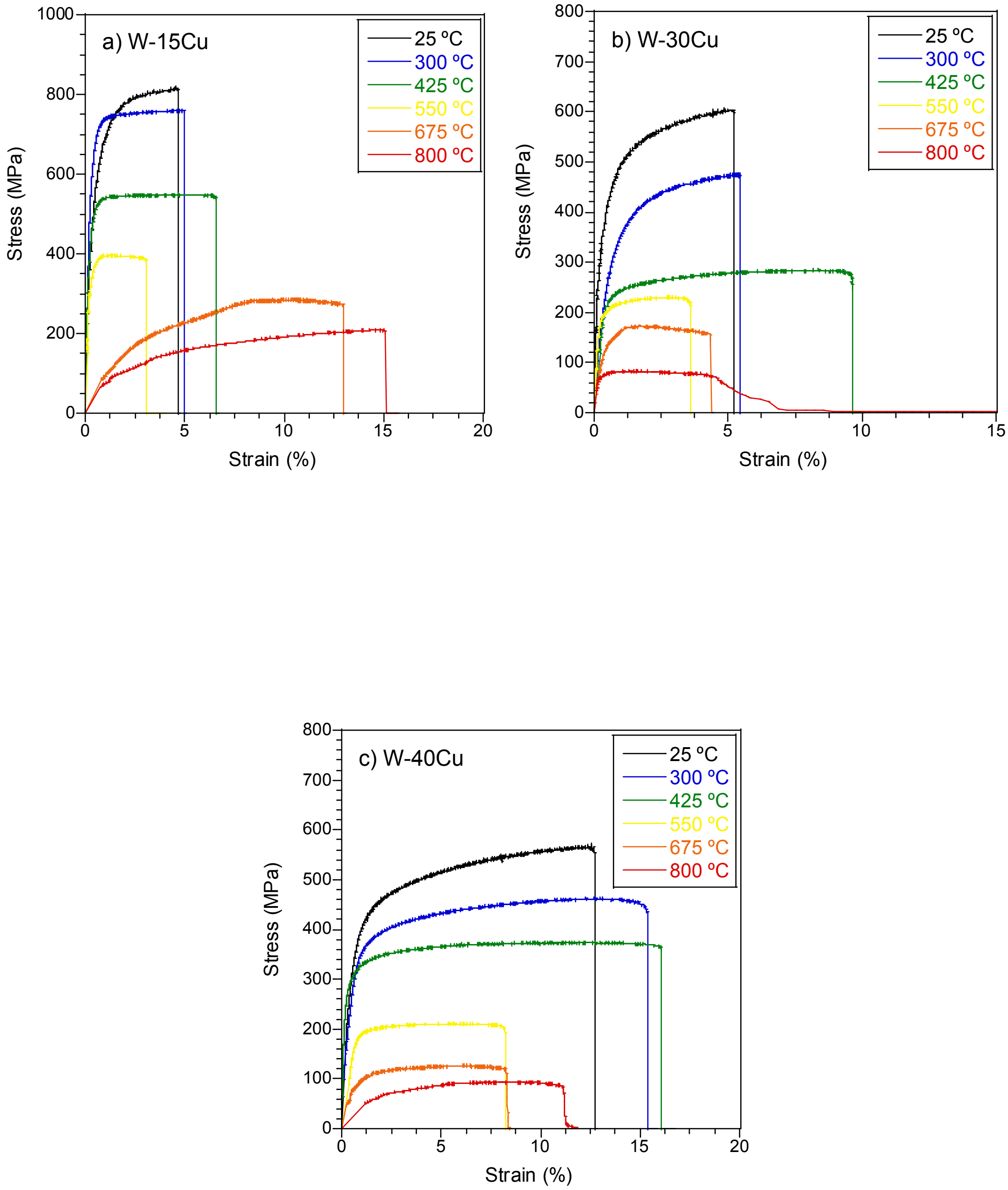

Fig. 4. True stress-strain curves of tensile tests for a) W-15Cu, b)W-30Cu and c)W-40Cu composites at different temperatures.

It is noticeable that the addition of Cu leads to a significant increase in ductility, though all materials exhibit ductile behaviour from room temperature. The curves display a characteristic nonlinear behaviour up to fracture, after the initial linear region, the curve shows a substantial nonlinear softening response until fracture occurs. The tensile elongation of W-15Cu composite increases with increasing temperature, while decreasing the true rupture stress, excepting the 550 ºC test shown. However, it should be noted that only one test has been represented for each temperature, though average values follow the general tendency observed at remaining temperatures. Zivelonghi [31] explained this scattering in the final rupture strain as a consequence of the random nature of the microstructure of tungsten-reinforced copper composites. On the contrary, both W-30Cu and W-40Cu exhibit the largest rupture strains at 425 ºC. At this temperature, the elongation of W-30Cu is indeed twice the one exhibited by W-15Cu (~5% strain vs 10% strain) and three times higher in the case of W-40Cu (~15% strain). However, the rupture strength at all temperatures were considerably lower compared to the latter (540 MPa, 380 MPa and 320 MPa at 425 ºC for W-15Cu, W-30Cu and W-40Cu, respectively).Tensile strength values can be better observed in Fig. 5 and Fig. 6 where yield strength at 0.2 % strain and the maximum strength are plotted as a function of temperature and composition.

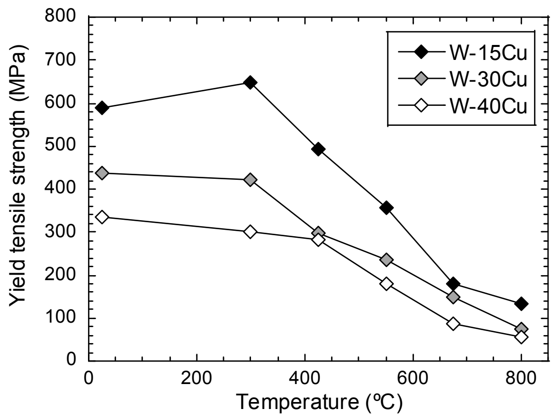

Fig. 5. Yield tensile strength of the composites as a function of composition and temperature

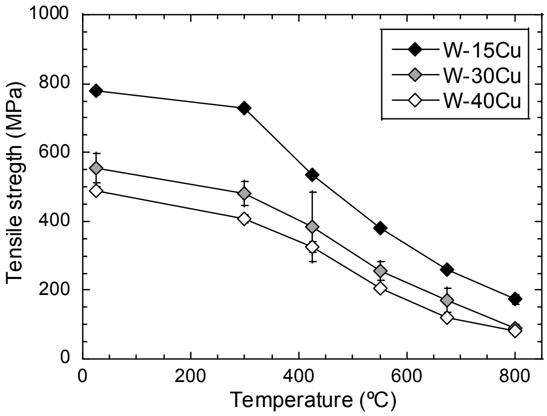

Fig. 6. Maximum tensile strength of the composites as a function of composition and temperature.

Both yield and maximum strength show similar trend for the three composites under study. The highest values of tensile strength are obtained at room temperature (780 MPa, 560 MPa and 500 MPa, for W-15Cu, W-30Cu and W-40Cu respectively) and almost stand at 300 ºC. Above this temperature they decrease uniformly down to 175 MPa for W-15Cu, and to 80 MPa at 800 ºC for W-30Cu and W-40Cu. However, tensile performance of W-30Cu is on average 18% higher than the observed for W-40Cu, but 40 % lower than for W-15Cu. Hence, the effect of Cu content on the tensile behaviour is evident. However, these differences are slightly higher in the case of yield strength (see Fig. 5), where the onset of plasticity observed at room temperature decreases from 600 MPa to 440 MPa and to 335 MPa as the weight percent of copper decreases from 15% to 30% and 40%, respectively.

These results are in accordance with observed in the fracture surfaces of the specimens. W-30Cu fractography can be better observed in[20], where a detailed study was performed. Fig. 7 (a-c) show the fracture surfaces of W-15Cu tests at different temperatures. At 25 ºC (Fig. 7 (a) inter- and transgranular cleavage of W grains indicates its brittle fracture while minor deformation of the Cu phase can be detected, consistent with the rupture strains observed in tensile curves (Fig. 4 (a)). At 550 ºC, some W residual grains still evidence flat and cleaved planes with elongated Cu phase around them. As testing temperature increases, so does the effect of Cu on the macroscopic performance of this composite. At the maximum temperature under test, the degradation of the material is evident: while W grains are rounded and inter-granular fracture is the dominant mode of rupture in the W skeleton, Cu phase is almost melted and its contribution to the tensile performance is quite low.

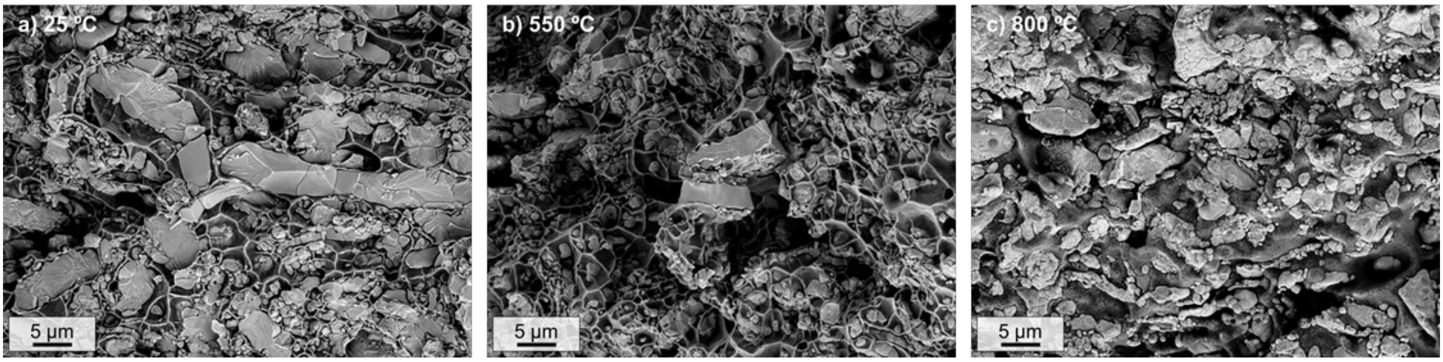

Fig. 7. SEM micrographs of the fractured surfaces of W–15Cu composite tested at a) 25 ºC, b) 550 ºC and c) 800 ºC.

The fracture surface of the material containing 40 wt.% Cu is quite different, compared with the composite containing 15 wt.% Cu, especially at 25 ºC (Fig. 8 (a)). Contiguity of W particles is rarely observable, in contrast with observed for the aforementioned composite. The deformation of the Cu phase is more prominent and particularly visible at 425 ºC (Fig. 8 (b)) with the characteristic dimples of a ductile fracture.

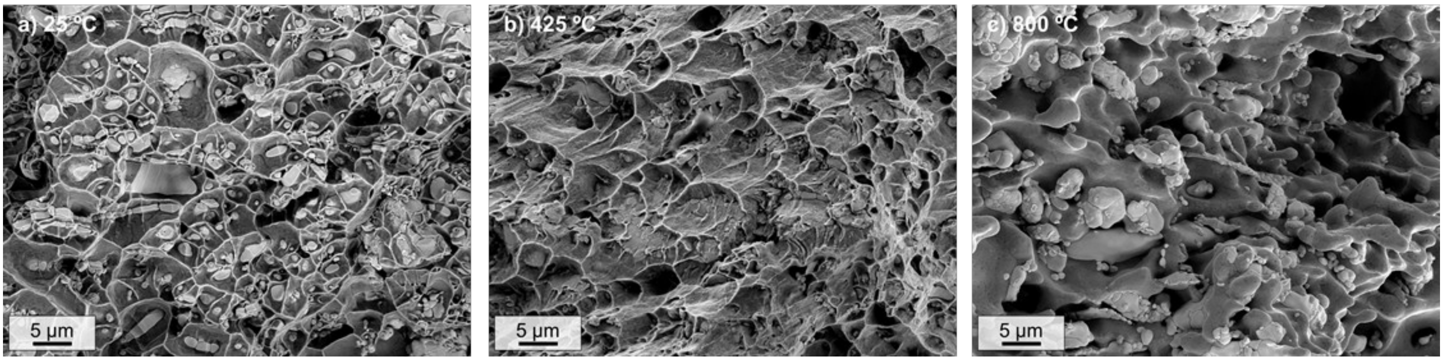

Fig. 8. SEM micrographs of the fractured surfaces of W–40Cu composite tested at a) 25 ºC, b) 425 ºC and c) 800 ºC.

- *Elastic modulus*

Load-deflection curves of the tests were used to calculate the modulus of elasticity by drawing a tangent to the steepest initial straight-line portion of it. Those data are also compared with literature values for W and Cu obtained from [32] and [33], respectively and represented in Fig. 9.

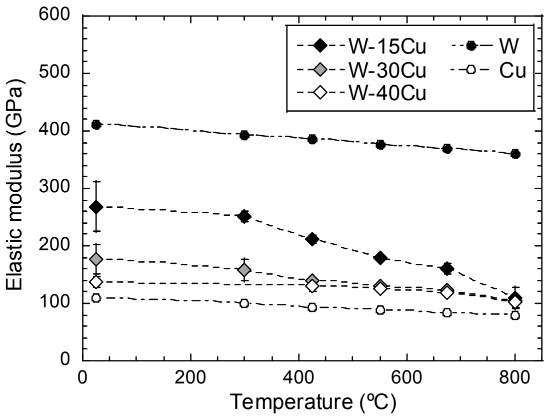

Fig. 9. Elastic modulus of W, Cu and W–Cu composites as a function of composition and temperature. Mean values and standard error.

The evolution of the elastic modulus with temperature for W-40Cu composite is quite similar to the observed for pure Cu, with a very small relative rate of change. On the contrary, as Cu content decreases, the different among the values obtained at RT, where they exhibit the highest, and at 800 ºC increases, since all the data converge at the same point (~105 GPa). At higher temperatures, the main contribution to the system stiffness comes from the W porous phase as Cu phase is already degraded.

For the better understanding, the values obtained at RT from the Strength Tests (ST) have been compared with those obtained via Resonance Frequency Analysis (RFA), both represented within the bounds predicted by the rules of mixtures, i.e. Voigt and Reuss models, in Fig. 10.

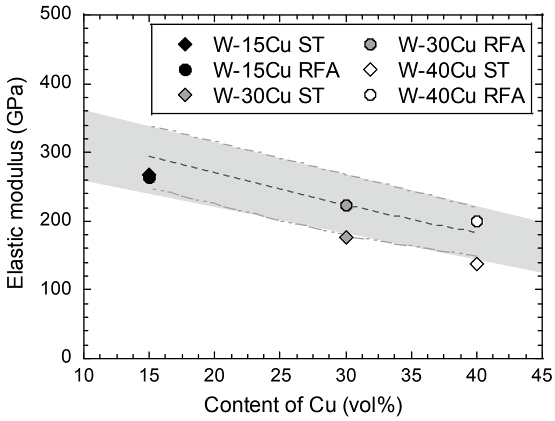

Fig. 10. Elastic modulus at RT of W/Cu composites as a function of composition, mean and standard error. Values were measured from the strength tests (ST) curves and by Resonant Frequency Analysis (RFA). Upper and lower bounds were estimated with the Voigt and Reuss models, respectively, while Hill model is the average of them.

As can be seen, in all cases the measured ST data are located between the area limited by the upper and lower bounds represented by the grey area. Furthermore, the data points are systematically closer to the lower bound, i.e. Reuss model, since Voigt bound clearly overestimates the stiffness. These data are in good agreement with observed by Hiraoka [34] for W-Cu composites produced by different routes. Totten and MacKenzie [35] explained the Reuss approach of elastic modulus in metal matrix composites by the hydrostatic stresses generated in the composite when the softer matrix phase is restrained from deformation by the hard particles.

- *Elastic modulus values obtained from RFA are significantly higher than those measured from ST when Cu content is higher than 30 wt.%. This observation has already been observed for Cu-based composites [36] and attributed to the sensitivity of RFA technique to the specimen dimensions and homogeneity [37].Coefficient of thermal expansion (CTE)*

Research performed by Arenz [38] found that a large number of polycrystalline and amorphous materials, W and Cu among them, obey the empirical relation $E = 4.5\ \alpha^{-2.3}$, where α is the uniaxial thermal expansion coefficient and E is the elastic modulus. Both properties are related intimately to lattice vibration, so energy well theory and thermodynamic analysis can be used to obtain a qualitative relationship.

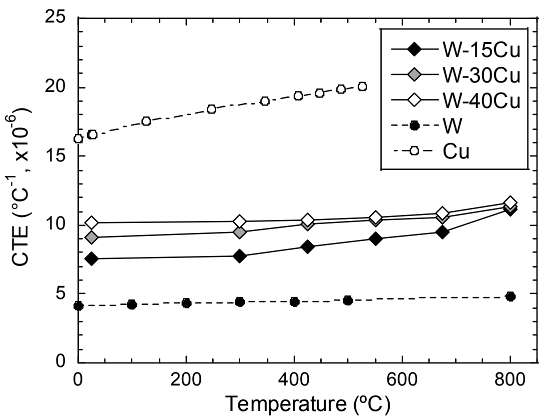

Fig. 11. Estimated coefficient of thermal expansion (CTE) versus temperature for investigated materials.

Arenz`s empirical relation was used to estimate the coefficient of thermal expansion (CTE) of the composites under study. The CTE versus temperature for pure tungsten, copper and W-Cu composites is illustrated in Fig. 11. One can notice that W–Cu composites, either W-15Cu or W-40Cu, show much lower CTE than that of pure copper and higher than that of pure tungsten. As expected, the CTE of W–Cu composites increases with the increase in copper content. However, as temperatures increases, this difference becomes smaller.

At room temperature, Duan and coworkers [39] measured experimentally the CTE of W-Cu composites produced by a similar route. Their results are in good agreement with the ones presented in Fig. 11. Furthermore, they treated the CTE of the composites as a weighted average of the thermal expansion of W and Cu in the sample, revealing that the variation tendency of measured values of CTE is the same as that of the theoretical ones, hence the same approach can be done with materials presented in this article.

In W–Cu composites, likewise elastic modulus, the high thermal expansion of Cu is constrained by the lower CTE of W particles. Therefore, the CTE of the composite is affected by the Cu distribution as well as the W-skeleton. At higher temperatures, when Cu is clearly degraded, the CTE is entirely controlled by the W structure, so all the materials tend to the same value (~ 11.5 10^{-6} $°C^{-1}$).

4. Conclusions

W-Cu composites were fabricated by means of liquid Cu infiltration of open porous W preforms in an industrially viable production route. Three different compositions have been compared in this investigation: W-15wt.% Cu, W-30wt.%Cu and W-40wt.%Cu.

The obtained microstructure has been found optimal for heat sink and thermal management applications. It presents high density, a homogeneous distribution of W particles forming a continuous structure, and a Cu phase located around it forming a interpenetrated network structure.

The mechanical properties (elastic modulus, fracture toughness and strength) of the composites show a palpable dependency on the Cu content; fracture mode changes from the dominantly brittle fracture of W particles with constrained deformation of the Cu phase at low Cu content (W-15Cu) to the predominance of the ductile fracture of Cu when its ratio is higher (W-40Cu). With the increase in temperature so does the contribution of the Cu phase to the rupture strain of the materials, although strong degradation is observed at 800 ºC. Meanwhile, there is no obvious growth of W particles. However, mechanical properties at operation temperatures, i.e. below 350 ºC, remain rather high, and even better than other materials reported previously, although slightly lower than the ones reported for W/CuCrZr composites [40]

CTE has been obtained between room temperature and 800 ºC from elastic modulus measurements. From these data, it is clear that the W skeleton determined the change in CTE, while the Cu network structure benefits the increase of thermal conductivity, as investigated by [21]. Furthermore, thermal properties can be tailored by controlling the porosity of the initial W preform, hence the composition of the final product.

The W-Cu composite materials presented in this paper would successfully drive away heat produced in the fusion chamber avoiding the mismatch between materials by tailoring CTE through the control of W skeleton porosity. What is more, these materials exhibit improved mechanical properties that can contribute to the structural support of the system. These facts are of vital importance to enhance the performance, life cycle and reliability of the heat sink components.

5. Acknowledgements

This work has been carried out within the framework of the EUROfusion Consortium and has received funding from the Euratom research and training programme 2014-2018 under grant agreement No 633053. The views and opinions expressed herein do not necessarily reflect those of the European Commission.

The authors also acknowledge the support of the Ministerio de Economía y Competitividad of Spain (research project MAT2015-70780-C4-4-P) and the Comunidad de Madrid (research project S2013/MIT-2862-MULTIMATCHALLENGE) who have funded this research.

References

[1] IAEA, "Technical basis for the ITER final design report, cost review and safety analysis (FDR)," Vienna, 1998.

[2] G. Pintsuk, V. Casalegno, M. Ferraris, T. Koppitz, and M. Salvo, "Thermal fatigue characterization of CFC divertor modules using a one step brazing process," *J. Nucl. Mater.*, vol. 426, no. 1–3, pp. 78–84, Jul. 2012.

[3] J. H. You *et al.*, "European DEMO divertor target: Operational requirements and material-design interface," *Nucl. Mater. Energy*, vol. 9, pp. 171–176, 2016.

[4] H. Greuner, A. Zivelonghi, B. Böswirth, and J. H. You, "Results of high heat flux testing of W/CuCrZr multilayer composites with percolating microstructure for plasma-facing components," *Fusion Eng. Des.*, vol. 98–99, no. APRIL, pp.

1310–1313, 2015.

[5] J.-H. H. You, “Copper matrix composites as heat sink materials for water-cooled divertor target,” *Nucl. Mater. Energy*, vol. 5, pp. 7–18, Dec. 2015.

[6] V. Barabash *et al.*, “Armor and heat sink materials joining technologies development for ITER plasma facing components,” *J. Nucl. Mater.*, vol. Volumes 28, no. Part 2, pp. 1248–1252, 2000.

[7] J. H. You and H. Bolt, “Analytical method for thermal stress analysis of plasma facing materials,” *J. Nucl. Mater.*, vol. 299, no. 1, pp. 9–19, Oct. 2001.

[8] G. Pintsuk, S. E. Brünings, J. E. Döring, J. Linke, I. Smid, and L. Xue, “Development of W/Cu-functionally graded materials,” *Fusion Eng. Des.*, vol. 66–68, pp. 237–240, 2003.

[9] Y. Itoh, M. Takahashi, and H. Takano, “Design of tungsten/copper graded composite for high heat flux components,” *Fusion Eng. Des.*, vol. 31, no. 4, pp. 279–289, 1987.

[10] S.-K. Joo, S.-W. Lee, and T.-H. Ihn, “Effect of cobalt addition on the liquid-phase sintering of W-Cu prepared by the fluidized bed reduction method,” *Metall. Mater. Trans. A*, vol. 25, no. 8, pp. 1575–1578, Aug. 1994.

[11] I. H. Moon, E. P. Kim, and G. Petzow, “Full Densification of Loosely Packed W–Cu Composite Powders,” *Powder Metall.*, vol. 41, no. 1, pp. 51–57, Jan. 1998.

[12] K. Daneshjou and M. Ahmadi, “Optimizing the effective parameters of tungsten - Copper composites,” *Trans. Can. Soc. Mech. Eng.*, vol. 30, no. 3, pp. 321–327,

2006.

[13] V. Barabash, "Current status and recent achievements in ITER materials/component fabrication and performance demonstration: vacuum vessel and in-vessel components," in *16th Intern. Conf. on Fusion Reactor Materials*, 2013.

[14] A. Elsayed, W. Li, O. A. El Kady, W. M. Daoush, E. A. Olevsky, and R. M. German, "Experimental investigations on the synthesis of W-Cu nanocomposite through spark plasma sintering," *J. Alloys Compd.*, 2015.

[15] X. Tang *et al.*, "Fabrication of W–Cu functionally graded material by spark plasma sintering method," *Int. J. Refract. Met. Hard Mater.*, vol. 42, pp. 193–199, Jan. 2014.

[16] M. Suarez *et al.*, "Challenges and Opportunities for Spark Plasma Sintering: A Key Technology for a New Generation of Materials," in *Sintering Applications*, InTech, 2013.

[17] A. G. Hamidi, H. Arabi, and S. Rastegari, "Tungsten-copper composite production by activated sintering and infiltration," *Int. J. Refract. Met. Hard Mater.*, 2011.

[18] J. L. Johnson, J. J. Brezovsky, and R. M. German, "Effect of liquid content on distortion and rearrangement densification of liquid-phase-sintered W-Cu," *Metall. Mater. Trans. A*, vol. 36, no. 6, pp. 1557–1565, Jun. 2005.

[19] S. Liang *et al.*, "Infiltrated W–Cu composites with combined architecture of hierarchical particulate tungsten and tungsten fibers," *Mater. Charact.*, vol. 110,

pp. 33–38, Dec. 2015.

[20] E. Tejado, A. v. Müller, J.-H. You, and J. Y. Pastor, “Evolution of mechanical performance with temperature of W/Cu and W/CuCrZrv composites for fusion heat sink applications,” *J. Nucl. Mater.*, 2017.

[21] A. v. Müller *et al.*, “Melt infiltrated tungsten–copper composites as advanced heat sink materials for plasma facing components of future nuclear fusion devices,” *Fusion Eng. Des.*, pp. 1–5, 2017.

[22] T. Palacios and J. Y. Pastor, “Influence of the notch root radius on the fracture toughness of brittle metals: Nanostructure tungsten alloy, a case study,” *Int. J. Refract. Met. Hard Mater.*, vol. 52, pp. 44–49, Sep. 2015.

[23] G. V. Guinea, J. Y. Pastor, J. Planas, and M. Elices, “Stress Intensity factor, compliance and CMOD for a General Three-Point-Bend Beam,” *Int. J. Fract.*, vol. 89, no. 2, pp. 103–116, 1998.

[24] ASTM Standard E1820-11, “Standard Test Method for Measurement of Fracture Toughness.” ASTM International, 2009.

[25] A. (Arun) Shukla, *Practical fracture mechanics in design*. Marcel Dekker, 2005.

[26] J. Blaber, B. Adair, and A. Antoniou, “Ncorr: Open-Source 2D Digital Image Correlation Matlab Software,” *Exp. Mech.*, vol. 55, no. 6, pp. 1105–1122, 2015.

[27] J. Cheng, L. Wan, Y. Cai, J. Zhu, P. Song, and J. Dong, “Fabrication of W–20wt. %Cu alloys by powder injection molding,” *J. Mater. Process. Technol.*, vol. 210, no. 1, pp. 137–142, Jan. 2010.

[28] L. Xu *et al.*, "Influence of copper content on the property of Cu-W alloy prepared by microwave vacuum infiltration sintering," *J. Alloys Compd.*, vol. 592, pp. 202–206, 2014.

[29] J. Kübier, "Fracture Toughness of Ceramics using the SEVNB Method: From a Preliminary Study to a Standard Test Method," in *Fracture Resistance Testing of Monolithic and Composite Brittle Materials*, 100 Barr Harbor Drive, PO Box C700, West Conshohocken, PA 19428-2959: ASTM International, 2002, pp. 93-93–14.

[30] A. Ibrahim, M. Abdallah, S. F. Mostafa, and A. A. Hegazy, "An experimental investigation on the W-Cu composites," *Mater. Des.*, 2009.

[31] A. Zivelonghi and J. H. You, "Mechanism of plastic damage and fracture of a particulate tungsten-reinforced copper composite: A microstructure-based finite element study," *Comput. Mater. Sci.*, vol. 84, pp. 318–326, 2014.

[32] J. M. Wheeler and J. Michler, "Invited Article: Indenter materials for high temperature nanoindentation," *Rev. Sci. Instrum.*, vol. 84, no. 10, p. 101301, Oct. 2013.

[33] J. R. Davis and ASM International, *Copper and copper alloys*. ASM International, 2001.

[34] Y. Hiraoka, T. Inoue, H. Hanado, and N. Akiyoshi, "Ductile-to-Brittle Transition Characteristics in W–Cu Composites with Increase of Cu Content," *Mater. Trans.*, vol. 46, no. 7, pp. 1663–1670, 2005.

[35] G. E. Totten and D. S. MacKenzie, *Handbook of aluminum*. Dekker, 2003.

[36] E. Tejado *et al.*, “New WC-Cu thermal barriers for fusion applications: high temperature mechanical behavior,” *J. Nucl. Mater.*, 2017.

[37] M. Radovic, E. Lara-Curzio, and L. Riester, “Comparison of different experimental techniques for determination of elastic properties of solids,” *Mater. Sci. Eng. A*, vol. 368, no. 1–2, pp. 56–70, 2004.

[38] R. J. J. Arenz, “Relation of Elastic Modulus to Thermal Expansion Coefficient in Elastic and Viscoelastic Materials,” *Sem*, no. 1, pp. 1–4, 2005.

[39] L. Duan, W. Lin, J. Wang, and G. Yang, “Thermal properties of W-Cu composites manufactured by copper infiltration into tungsten fiber matrix,” *Int. J. Refract. Met. Hard Mater.*, vol. 46, pp. 96–100, 2014.

[40] J.-H. H. You, A. Brendel, S. Nawka, T. Schubert, and B. Kieback, “Thermal and mechanical properties of infiltrated W/CuCrZr composite materials for functionally graded heat sink application,” *J. Nucl. Mater.*, vol. 438, no. 1–3, pp. 1–6, 2013.